

# Theoretical study of the decomposition of ethyl and ethyl 3-phenyl glycidate

D. Josa<sup>[a]</sup>, A. Peña-Gallego<sup>\*,[a]</sup>, J. Rodríguez-Otero<sup>[a]</sup> and E.M. Cabaleiro-Lago<sup>[b]</sup>

[a] *Departamento de Química Física, Facultad de Química, Universidad de Santiago de Compostela, Avda. das Ciencias, s/n 15782 Santiago de Compostela, Spain.*

[b] *Departamento de Química Física, Facultad de Ciencias, Universidad de Santiago de Compostela, Campus de Lugo. Avda. Alfonso X El Sabio, s/n 27002 Lugo, Spain.*

e-mail: angeles.pena@usc.es

## Abstract

The mechanism of the decomposition of ethyl and ethyl 3-phenyl glycidate in gas phase has been studied by density functional theory (DFT) and MP2 methods. A proposed mechanism for the reaction indicates that the ethyl side of the ester is eliminated as ethylene through a concerted six-membered cyclic transition state, and the unstable intermediate glycidic acid rapidly decarboxylates to give the corresponding aldehyde. Two possible pathways for glycidic acid decarboxylation were studied, one of them via a five-membered cyclic transition state and the other one via a four-membered cyclic transition state. The results of the calculations indicate that the decarboxylation reaction occurs via a mechanism with five-membered cyclic transition state.

KEYWORDS: ethyl glycidate, ethyl 3-phenyl glycidate, *ab initio* calculations, DFT calculations, reaction mechanism

## Introduction

One of the most important transformations of glycidic esters is their decarboxylation to give aldehydes and ketones. Various methods for this conversion have been studied experimentally.<sup>1-5</sup> However, an accurate description of this mechanism is a challenging task, since the glycidic acid intermediate decomposes even at room temperature.

According to experimental studies performed by Chuchani and co-workers<sup>6</sup> the reaction of the decomposition of ethyl 3-phenyl glycidate is homogeneous, unimolecular and obeys a first-order rate law. The results of this investigation indicate that the reaction occurs in two steps: the first step of the mechanism involves the elimination of the alkyl side of the ester through a concerted six-membered cyclic transition state; the second step involves the decarboxylation of glycidic acid. Two pathways were proposed for this step. One of them via a five-membered cyclic transition state (Figure 1, path I) and the other via a four-membered cyclic transition state (Figure 1, path II).<sup>6</sup>

In reaction mechanisms with similar steps, as in the elimination of the ethyl carbonates<sup>7</sup> and ethyl carbamates<sup>8-10</sup>, the decarboxylation process in the second step occurs via a four-membered cyclic transition state. However, according to experiments, a four-membered cyclic transition state appears to be unlikely for the glycidic acid studied because the epoxy intermediate was not isolated. A mechanism suggested for decarboxylation is that the carbon at 3-position, rather than the carbon at 2-position, is more liable to a C-O bond polarization, in the sense of  $C^{\delta+} \dots O^{\delta-}$ . So, the oxygen becomes very nucleophilic and may abstract the hydrogen of the COOH through a five-membered cyclic transition state to yield 2-phenylacetaldehyde and carbon dioxide (Figure 1, path I).<sup>6</sup>

The final product, 2-phenylacetaldehyde, is an important intermediate used in the preparation of the novel active substances of insecticides, herbicides, fungicides, and medicines.<sup>11</sup> It is also found in many foods and flowers.<sup>12-13</sup>

Although the studies performed by Chuchani *et al.*<sup>6</sup> allow us to rationalize a mechanism for the decarboxylation of glycidic acid, a detailed study of the mechanism taking into account the two possible pathways for the glycidic acid decarboxylation to confirm their experimental hypothesis is necessary.

Therefore, the goal of this work is to perform an accurate theoretical study of the decomposition of ethyl 3-phenyl glycidate in order to explore the nature of reaction mechanism. Geometries of the different reactants, products and intermediates were optimized at different levels of calculation. The vibrational frequencies were calculated at the same level. IRC's calculations were performed and the progress of the reaction was followed employing the Wiberg bond indices<sup>14</sup>. Activation energies and Gibbs free energies of activation have also been analyzed.

## **Computational Details**

The mechanisms of the decomposition of ethyl and ethyl 3-phenyl glycidate in the gas phase were investigated by means of electronic structure calculations. The geometry of each stationary point corresponding to reactants, products, and transition states was optimized employing second-order Møller-Plesset theory (MP2) or DFT using the B3LYP functional.

Other studies<sup>15</sup> indicate an important improvement in the results adding diffuse functions. Therefore, all calculations in this work include diffuse functions. The 6-31+G\*, 6-31++G\*\*, aug-cc-pVDZ and aug-cc-pVTZ basis set were employed in the calculations.

Single point calculations at the MP4 and CCSD(T) levels were also done for selected conformations for the study of the decomposition of ethyl glycidate.

All points were characterized as minima or transition structures by calculating the harmonic frequencies and forces constants, using analytical second derivatives. Zero point-energy (ZPE) corrections were included in the calculations.

Intrinsic reaction coordinate (IRC) calculations<sup>16</sup> were also performed to follow the reaction path in both directions from transition states at the B3LYP/6-31+G\* level of theory.

The activation energy  $E_a$  was obtained using the following equations:

$$E_a = \Delta H^\ddagger(T) + RT$$

$$\Delta H^\ddagger = \Delta H_{TS} - \Delta H_{react}$$

where  $\Delta H_{TS}$  and  $\Delta H_{react}$  are the enthalpies for the transition state and the reactants (reactive conformation), respectively.  $R$  represents the universal gas constant (1.9872 cal mol<sup>-1</sup> K<sup>-1</sup>), and  $T$  represents the temperature (we have used a value of 643.15 K, temperature where there are experimental kinetic data).<sup>6</sup>

Natural bond orbital (NBO) analysis was performed using the NBO program, implemented in the Gaussian03 program package<sup>17</sup> to follow the progress of the reactions and investigate the bonding characteristics. All calculations were carried out using the Gaussian03 program package.<sup>17</sup>

## Results and Discussion

The mechanism proposed in experimental studies<sup>6</sup> for the reaction of the decomposition of ethyl 3-phenyl glycidate in the gas phase is given in Figure 1. The reaction has two steps: the first process occurs via a six-membered cyclic transition state (TS1) and the second one can occur via a five or four-membered cyclic transition

state, given as TS2 and TS3, respectively.<sup>6</sup> These two possible pathways for the decomposition of ethyl 3-phenyl glycidate were investigated in this work. In order to evaluate the validity of the results obtained for the decomposition of ethyl 3-phenyl glycidate, a preliminary study was performed at the same theoretical level and compared with high level *ab initio* calculations.

Several optimizations using different starting points were performed at the MP2/6-31+G\* level to obtain the ethyl glycidate minima. Figure 2 shows the geometries for the two most important located minima. The minimum II with a planar skeleton corresponds with the most stable structure found in the exploration of the minima for ethyl glycidate. This minimum is 0.19 kcal/mol (ZPE corrections included) more stable than the minimum I. However, the minimum I was used in the following calculations due to it having a more favorable geometry for the elimination of the alkyl side of the ester through a concerted six-membered cyclic transition state.

Geometrical parameters for reactants and transition states for the reaction studied are given in Table 1. The numeration of the atoms involved in the reaction of the decomposition of ethyl and ethyl 3-phenyl glycidate is depicted in Figure 3.

In general, little changes are observed in the bond distances comparing the calculations at different levels. The most relevant change observed was in the H<sub>9</sub>-O<sub>5</sub> and O<sub>6</sub>-C<sub>7</sub> bond in the transition state for the reaction of the decomposition of ethyl and ethyl 3-phenyl glycidate, respectively (see Table 1).

The change of basis set provides a more significant difference in the H<sub>9</sub>-O<sub>5</sub> bond of ethyl glycidate than the change of method, for example, a decrease of the 0.086 Å is observed in the calculations using MP2 method with aug-cc-pVDZ compared to 6-31+G\* basis set. On the other hand, the calculations employing MP2 compared to B3LYP with 6-31+G\* basis set produce more change in the O<sub>6</sub>-C<sub>7</sub> bond of ethyl

3-phenyl glycidate compared to the increase of the basis set size. A decrease of the 0.061 Å was obtained in this case.

**Table 1.** Main distances (Å) in reactants and transition states for the rate-determining step for decomposition of ethyl glycidate (TS2) and ethyl 3-phenyl glycidate (TS1) at different calculation levels.

	B3LYP/6-31+G*		B3LYP/6-31++G**		MP2/6-31+G*		MP2/aug-cc-pVDZ	
	R	TS	R	TS	R	TS	R	TS
Ethyl glycidate								
C <sub>1</sub> -O <sub>2</sub>	1.438	1.991	1.438	2.000	1.449	2.009	1.458	2.024
O <sub>2</sub> -H <sub>9</sub>	2.065	1.033	2.069	1.042	2.031	1.039	2.017	1.048
H <sub>9</sub> -O <sub>5</sub>	0.980	1.632	0.976	1.557	0.985	1.616	0.979	1.530
O <sub>5</sub> -C <sub>4</sub>	1.349	1.256	1.348	1.259	1.353	1.256	1.357	1.260
C <sub>4</sub> -C <sub>3</sub>	1.511	1.648	1.510	1.649	1.504	1.695	1.509	1.701
C <sub>3</sub> -C <sub>1</sub>	1.476	1.425	1.476	1.424	1.471	1.401	1.480	1.406
C <sub>3</sub> -O <sub>2</sub>	1.440	1.447	1.439	1.442	1.450	1.454	1.457	1.457
Ethyl 3-phenyl glycidate								
O <sub>5</sub> -C <sub>4</sub>	1.212	1.277	1.213	1.275	1.222	1.285		
C <sub>4</sub> -O <sub>6</sub>	1.349	1.266	1.349	1.268	1.354	1.275		
O <sub>6</sub> -C <sub>7</sub>	1.454	2.086	1.454	2.048	1.458	2.025		
C <sub>7</sub> -C <sub>8</sub>	1.521	1.401	1.521	1.404	1.515	1.398		
C <sub>8</sub> -H <sub>9</sub>	1.094	1.309	1.093	1.309	1.092	1.305		
H <sub>9</sub> -O <sub>5</sub>	2.909	1.335	2.913	1.324	2.723	1.327		

It seems that B3LYP overestimates the O<sub>6</sub>-C<sub>7</sub> bond distance in the transition state compared with MP2, it may be due to the lack of ability of B3LYP functional to treat long range interactions, as discussed in the previous study.<sup>15</sup>

All calculations indicate TS1 structures very distant from the planarity in the first step of reaction. A maximum deviation of 40° and 39° was observed at the

MP2/6-31+G\* level for O<sub>5</sub>-C<sub>4</sub>-O<sub>6</sub>---C<sub>7</sub> dihedral angle of ethyl glycidate and ethyl 3-phenyl glycidate, respectively (see Table 2).

**Table 2.** Dihedral angles (degrees) around the six-membered cyclic transition state (TS1) for the decomposition of ethyl and ethyl 3-phenyl glycidate.

	C <sub>4</sub> O <sub>6</sub> C <sub>7</sub> C <sub>8</sub>	O <sub>5</sub> C <sub>4</sub> O <sub>6</sub> C <sub>7</sub>	O <sub>6</sub> C <sub>4</sub> O <sub>5</sub> H <sub>9</sub>	C <sub>4</sub> O <sub>5</sub> H <sub>9</sub> C <sub>8</sub>	O <sub>5</sub> H <sub>9</sub> C <sub>8</sub> C <sub>7</sub>	H <sub>9</sub> C <sub>8</sub> C <sub>7</sub> O <sub>6</sub>
Ethyl glycidate						
B3LYP/6-31+G*	-6.0	20.9	-19.8	-2.9	15.5	-4.7
B3LYP/6-31++G**	-5.0	20.7	-20.1	-1.2	14.6	-5.4
MP2/6-31+G*	-13.2	39.6	-35.7	-7.0	27.9	-7.1
MP2/aug-cc-pVDZ	-9.6	37.2	-34.8	-5.3	27.6	-9.2
Ethyl 3-phenyl glycidate						
B3LYP/6-31+G*	-5.5	19.7	-18.7	-3.3	15.3	-4.6
B3LYP/6-31++G**	-4.7	19.5	-19.0	-1.5	14.2	-5.2
MP2/6-31+G*	-12.8	38.6	-34.9	-6.6	27.1	-6.9

In general ethyl 3-phenyl glycidate has a slightly smaller out of plane compared to ethyl glycidate. As can be seen in Table 2, the level of calculation has a large influence on the out of plane for TS1. The calculation using MP2 method provides much large out of plane for TS1 than the B3LYP with 6-31+G\* basis set. The maximum difference observed is about 19° for the O<sub>5</sub>-C<sub>4</sub>-O<sub>6</sub>---C<sub>7</sub> dihedral angle. The importance of an accurate level of calculation was described in previous theoretical studies for similar mechanisms;<sup>15</sup> where a transition state was observed very distant from planarity at the MP2 level, while Erickson *et al.*<sup>18</sup> had predicted a fully planar transition state employing Hartree-Fock calculations.

In addition, the degree of lengthening of the two bonds that are breaking in the TS1 was analyzed to obtain the percentage of bond lengthening between the transition

state and reactant in order to evaluate concerted reaction rates for the first step of reaction for ethyl and ethyl 3-phenyl glycidate, the results are shown in Table 3.

**Table 3.** Bond lengths (Å) of the O<sub>6</sub>-C<sub>7</sub> and C<sub>8</sub>-H<sub>9</sub> in the reactant and the transition state for the first step of the decomposition of ethyl and ethyl 3-phenyl glycidate at different calculation levels<sup>a</sup>.

		O <sub>6</sub> -C <sub>7</sub>	C <sub>8</sub> -H <sub>9</sub>	P (O <sub>6</sub> -C <sub>7</sub> )	P (C <sub>8</sub> -H <sub>9</sub> )
Ethyl glycidate					
B3LYP/6-31+G*	react	1.45410	1.09431	43.4	19.6
	TS1	2.08592	1.30859		
B3LYP/6-31++G**	react	1.45471	1.09323	40.9	19.6
	TS1	2.04918	1.30750		
MP2/6-31+G*	react	1.45809	1.09211	38.9	19.4
	TS1	2.02480	1.30435		
MP2/aug-cc-pVDZ	react	1.46022	1.09894	34.5	20.2
	TS1	1.96417	1.32065		
Ethyl 3-phenyl glycidate					
B3LYP/6-31+G*	react	1.45387	1.09441	43.5	19.6
	TS1	2.08584	1.30957		
B3LYP/6-31++G**	react	1.45448	1.09333	40.8	19.7
	TS1	2.04849	1.30888		
MP2/6-31+G*	react	1.45838	1.09222	38.8	19.5
	TS1	2.02465	1.30539		

<sup>a</sup> Percent of lengthening between the transition state and the reactant bond (results given

in percent):  $P(l) = (l_{TS} - l_{react}) / (l_{react})$ .



Our result is in agreement with the studies obtained by Hermida-Rámon *et al.*<sup>15</sup> As can be observed from Table 3, the MP2 method decreases the difference of the values of the percentage of O<sub>6</sub>-C<sub>7</sub> and C<sub>8</sub>-H<sub>9</sub> bond lengths compared to B3LYP, especially employing the aug-cc-pVDZ basis set for the elimination of ethyl glycidate, indicating a more concerted process. These results may be due to overestimation of the length of the O<sub>6</sub>-C<sub>7</sub> bond in the transition state by B3LYP functional discussed above. The study for ethyl 3-phenyl glycidate shows similar results.

The calculated activation energy and Gibbs free energy of activation for the transition states analyzed are summarized in Table 4. The calculations were performed to the same temperature used in the experiments, 643.15K.<sup>6</sup> The calculated values of the activation energy and Gibbs free energy of activation for the decomposition of ethyl 3-phenyl glycidate, agree well with the experimental data.<sup>6</sup>

It can be seen from Table 4 that the reaction of ethyl glycidate and ethyl 3-phenyl glycidate despite having similar TS1 activation energy values, shows significant differences in the TS2 values. The introduction of phenyl group in the 3-position in the ethyl glycidate provides a stabilization of the 17.4 kcal/mol for TS2 activation energy at the MP2/6-31+G\* level. This result may be due to a stabilization of the carbocation character of the carbon at the 3-position of glycidic acid intermediate by resonance. The  $\pi$  electrons of the phenyl group help delocalize the positive charge, increasing the stability. Therefore, the rate-determining step for the decomposition of ethyl 3-phenyl glycidate is the TS1, while the TS2 is the rate-determining step in the decomposition of ethyl glycidate.

Imaginary frequencies of the 1535.2i and 1069.4i cm<sup>-1</sup> were obtained for decomposition of ethyl 3-phenyl glycidate (TS1) and ethyl glycidate (TS2),

respectively, at the MP2/6-31+G\* level. The optimized transition structures for the decomposition of ethyl 3-phenyl glycidate are given in Figure 4.

**Table 4.** Activation energy and Gibbs free energy of activation in kcal/mol at 643.15 K for the decomposition of ethyl and ethyl 3-phenyl glycidate at different calculation levels.

Geometry and vibrational calculation	Single point energy	TS1		TS2		TS3	
		$E_a$	$\Delta G^\ddagger$	$E_a$	$\Delta G^\ddagger$	$E_a$	$\Delta G^\ddagger$
Ethyl glycidate							
B3LYP/6-31+G*	B3LYP/6-31+G*	46.83	45.36	49.58	48.45	65.98	64.49
B3LYP/6-31++G**	B3LYP/6-31++G**	44.62	43.44	49.03	47.97	65.38	63.98
MP2/6-31+G*	MP2/6-31+G*	52.64	51.72	60.33	58.81	67.84	66.56
	MP4/6-31+G*	51.85	55.60	55.20	49.70	67.91	71.29
MP2/aug-cc-pVDZ	MP2/aug-cc-pVDZ	48.31	47.41	58.55	57.27	64.54	63.08
	MP4/aug-cc-pVDZ	47.71	51.12	53.29	55.20	64.49	67.81
	MP4/aug-cc-pVTZ	48.45	51.87	55.00	56.91	63.86	67.18
	CCSD(T)/aug-cc-pVDZ	48.70	55.47	53.55	55.47	68.21	71.53
Ethyl 3-phenyl glycidate							
B3LYP/6-31+G*	B3LYP/6-31+G*	46.91	45.50	32.08	32.65	63.99	62.86
B3LYP/6-31++G**	B3LYP/6-31++G**	44.70	43.58	31.45	31.91	64.25	62.74
MP2/6-31+G*	MP2/6-31+G*	52.68	51.73	42.93	42.83	66.49	65.19
Experimental <sup>a</sup> (643.15 K)		45.43 ±1.39	48.35				

<sup>a</sup> Experimental data for the decomposition of ethyl 3-phenyl glycidate (Ref 6).

The comparison of the results at different calculation levels given in Table 4 provides similar observations than those obtained in the theoretical study of the thermal elimination of ethyl formate.<sup>15</sup> Therefore, our results confirm that the previous study employing the small molecule of ethyl formate at different level calculations is a good reference for other similar theoretical studies of bigger molecules.

The calculation at the B3LYP/6-31++G\*\* level for ethyl 3-phenyl glycidate gives an activation energy of only 0.73 kcal/mol lower than the experimental value for the rate-determining step (TS1). However, as we have discussed above, the lack ability of the B3LYP functional to treat long range interactions produces the overestimation of the O<sub>6</sub>-C<sub>7</sub> bond distance in the transition state. Moreover, the DFT transition state is more planar than the MP2 ones.

Free energy profile for the process of decomposition of ethyl 3-phenyl glycidate is depicted in Figure 5. It can be clearly observed that the second step of the mechanism occurs via a five-membered cyclic transition state (TS2). The other pathway with a four-membered cyclic transition state (TS3) shows a activation free energy 22.36 kcal/mol higher than the corresponding values for TS2 at the MP2/6-31+G\* level. Our theoretical results confirm the previous experimental hypothesis that the second step of the mechanism occurs by a five-membered cyclic transition state.<sup>6</sup>

Wiberg bond indices<sup>14</sup> were computed to obtain a detailed analysis of the progress of the reaction. Table 5 summarizes the Wiberg bond indices corresponding to the bonds involved in the reaction center for the rate-determining step of the decomposition of ethyl and ethyl 3-phenyl glycidate.

The bond breaking and bond forming process along the reaction path can be analyzed employing the synchronicity (*Sy*) concept proposed by Moyano *et al.*<sup>19</sup> The synchronicity values vary between zero and one, which is the case when all bonds

involved in the reaction have broken or formed at exactly the same extent in the transition state. The ( $S_y$ ) can be calculated by means of the expression:

$$S_y = 1 - A$$

where  $A$  is the asynchronicity, calculated as:

$$A = \frac{1}{(2N - 2)} \sum \frac{|\delta B_i - \delta B_{av}|}{\delta B_{av}}$$

and where  $n$  is the number of bonds directly involved in a reaction chemical.

The relative variation of bond index is given by:

$$\delta B_i = \frac{(B_i^{TS} - B_i^R)}{(B_i^P - B_i^R)}$$

where the superscripts  $R$ ,  $TS$  and  $P$  refer to reactants, transition states and products, respectively.

The percentage evolution ( $\%EV$ )<sup>20</sup> of the bond order is calculated as:

$$\%EV = 100\delta B_i$$

The average value,  $\delta B_{av}$ , is obtained from:

$$\delta B_{av} = \frac{1}{n} \sum \delta B_i$$

The calculated Wiberg bond indices for the rate-determining step for the decomposition of ethyl 3-phenyl glycidate indicate a more advanced progress in the  $O_6-C_7$  bond breaking (63%) and less progress in the  $C_7-C_8$  double bond formation (39%).

The synchronicity value of the 0.92, indicates a slightly asynchronous process. The charge distribution in reactants and transition states obtained in the NBO analysis results are given in Table 6. It can be seen that there is a significant positive charge developed in the transition states compared with reactants on  $H_9$  (from 0.25 in R to 0.42 in TS) and an increase in the negative charge of  $O_5$  (from -0.60 in R to -0.68 in TS), this

negative character of O<sub>5</sub> allows the H<sub>9</sub> abstraction in the transition state, and an increase in the negative charge in O<sub>6</sub> (from -0.55 in R to -0.63 in TS) following the breaking of the O<sub>6</sub>-C<sub>7</sub> bond. The results indicate that the polarization of the O<sub>6</sub>-C<sub>7</sub> bond is an important factor in the decomposition of ethyl 3-phenyl glycidate.

**Table 5.** Wiberg bond indices ( $B_i$ ) of reactants, transition states and products for the rate-determining step of the reaction of the decomposition of ethyl and ethyl 3-phenyl glycidate, percentage of evolution ( $\%EV$ ) through the chemical process of the bond indices at the transition states, degree of advancement of the transition states ( $\delta B_{av}$ ), and absolute synchronicities ( $S_y$ ). Values obtained at B3LYP/6-31+G\* level.

Analysis of the progress of the reaction								
Ethyl glycidate								
	C <sub>1</sub> -O <sub>2</sub>	O <sub>2</sub> -H <sub>9</sub>	H <sub>9</sub> -O <sub>5</sub>	O <sub>5</sub> -C <sub>4</sub>	C <sub>4</sub> -C <sub>3</sub>	C <sub>3</sub> -C <sub>1</sub>	$\delta B_{av}$	$S_y$
$B_i^R$	0.9053	0.0294	0.6809	1.0627	0.9659	0.9868	0.493	0.754
$B_i^{TS2}$	0.4198	0.5578	0.1374	1.4334	0.7556	1.1798		
$B_i^P$	0.0000	0.7317	0.0000	1.8920	0.0000	1.9086		
$\%EV$	53.63	75.24	79.82	44.70	21.77	20.94		
Ethyl 3-phenyl glycidate								
	O <sub>5</sub> -C <sub>4</sub>	C <sub>4</sub> -O <sub>6</sub>	O <sub>6</sub> -C <sub>7</sub>	C <sub>7</sub> -C <sub>8</sub>	C <sub>8</sub> -H <sub>9</sub>	H <sub>9</sub> -O <sub>5</sub>	$\delta B_{av}$	$S_y$
$B_i^R$	1.7373	1.0461	0.8516	1.0332	0.9204	0.0009	0.508	0.922
$B_i^{TS1}$	1.3617	1.4302	0.3135	1.4257	0.4493	0.2930		
$B_i^P$	1.0608	1.7669	0.0000	2.0429	0.0000	0.6814		
$\%EV$	55.5	53.3	63.2	38.9	51.2	42.92		

The reaction of decomposition of ethyl glycidate with a five-membered cyclic transition state show a more advanced progress in the H<sub>9</sub>-O<sub>5</sub> bond breaking (80%), the bond formation of O<sub>2</sub>-H<sub>9</sub> (75%) also shows a very large progress in the reaction

mechanism. Therefore, the results indicate that the transference of H<sub>9</sub> is the most important process in the mechanism of decomposition of ethyl glycidate. The breaking of the C<sub>3</sub>-C<sub>1</sub> and C<sub>4</sub>-C<sub>3</sub> bonds are the less advanced processes.

This mechanism shows a synchronicity value of 0.75, indicating a more asynchronous process compared with the mechanism of the decomposition of the ethyl 3-phenyl glycidate. Natural bond orbital (NBO) charge analysis reveals that C<sub>1</sub> becomes more positive in the transition state (from -0.13 in R to -0.01 in TS), while C<sub>3</sub> becomes more negative (from -0.07 in R to -0.14 in TS). Therefore, the results indicate that C<sub>1</sub> and not C<sub>3</sub> is responsible for the increase of O<sub>2</sub> nucleophilicity (from -0.55 in R to -0.64 in TS) to allow the abstraction of H<sub>9</sub> of the COOH, in agreement with the results rationalized by Chuchani *et al.* for 3-phenylglycidic acid decarboxylation.<sup>6</sup>

**Table 6.** NBO charges, calculated at the B3LYP/6-31+G\* level, at the atom involved in the reaction center for the rate-determining step for the reaction of the decomposition of ethyl and ethyl 3-phenyl glycidate.

NBO charges						
Ethyl glycidate						
	C <sub>1</sub>	O <sub>2</sub>	H <sub>9</sub>	O <sub>5</sub>	C <sub>4</sub>	C <sub>3</sub>
react	-0.12690	-0.55526	0.52251	-0.70862	0.77193	-0.06642
TS2	-0.00777	-0.64257	0.53812	-0.66522	0.78554	-0.14463
Ethyl 3-phenyl glycidate						
	O <sub>5</sub>	C <sub>4</sub>	O <sub>6</sub>	C <sub>7</sub>	C <sub>8</sub>	H <sub>9</sub>
react	-0.59938	0.78226	-0.55390	-0.13623	-0.71790	0.25070
TS1	-0.67882	0.79276	-0.63049	-0.11493	-0.81660	0.42491

## Conclusions

The decomposition of ethyl and ethyl 3-phenyl glycidate was studied by density functional theory (DFT) and MP2 methods for an accurate study of the nature of the reaction mechanism. The calculations indicate that the six-membered transition state in the first step of the reaction has a non-planar structure and the reaction process through an asynchronous concerted mechanism. The second step of the mechanism comprising the decarboxylation of glycidic acid occurs via a five-membered cyclic transition state; the other pathway via a four-membered cyclic transition state proposed for this step by experiments<sup>6</sup> shows Gibbs free energy of activation 22.36 kcal/mol higher than the pathway via a five-membered cyclic transition state at the MP2/6-31+G\* level.

Although the first step of both reactions studied in this work is very similar, significant differences in the second step are observed. The transition state of the decarboxylation of 3-phenylglycidic acid has a special stabilization produced by the phenyl group. Therefore, the rate-determining step for the decomposition of ethyl 3-phenyl glycidate is the TS1, while the rate-determining step for the decomposition of ethyl glycidate is the TS2.

The evaluation at different calculation levels indicates similar results than described in the previous theoretical study for the thermal elimination of ethyl formate.<sup>15</sup> The use of a method including the electronic correlation and diffuse basis set is fundamental for a good description of the studied systems.

Theoretical results for activation energy show a good agreement with experimental value. The calculated percentages of evolution of the bonds involved in the reaction indicate that the O<sub>6</sub>-C<sub>7</sub> bond breaking for ethyl 3-phenyl glycidate and the H<sub>9</sub>-O<sub>5</sub> bond breaking for ethyl glycidate are the most advanced processes for the reactions in the transition states.

## **Acknowledgments**

The authors want to express their gratitude to the CESGA (Centro de Supercomputación de Galicia) for the use of their computers. D. J. thanks the Spanish Ministry of Education for FPU scholarship.



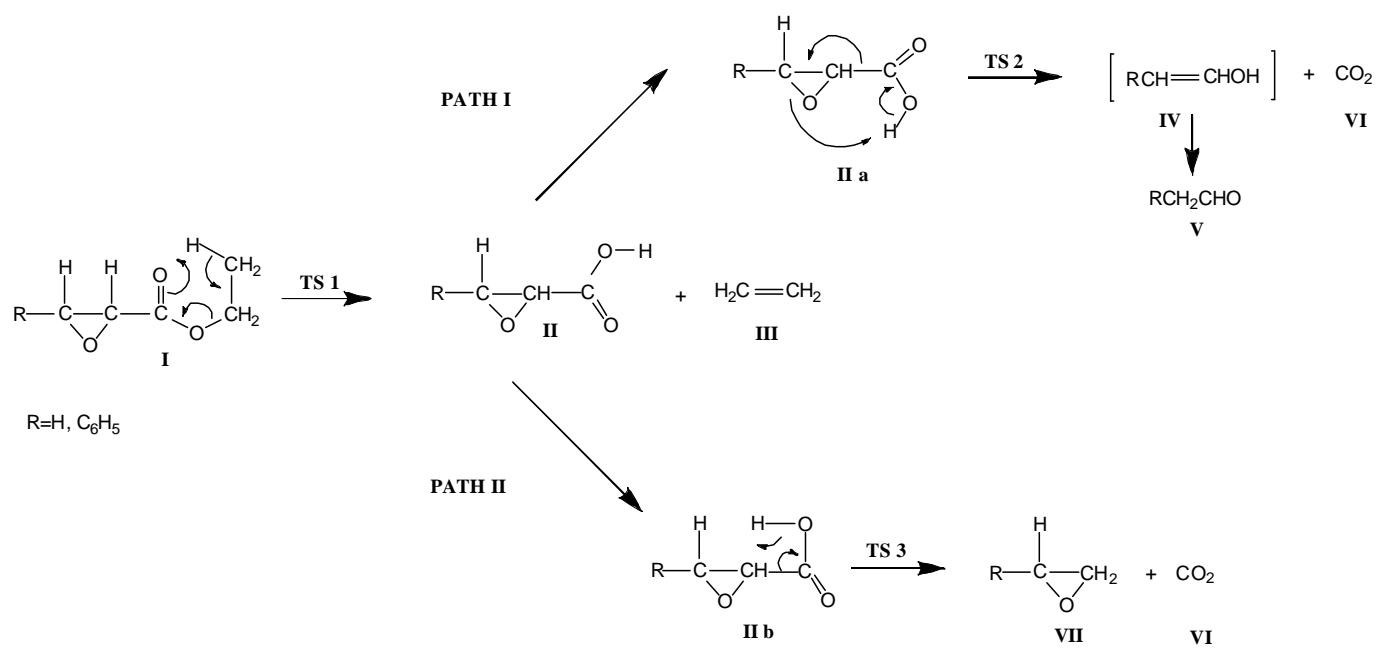


**Figure 1.** Two mechanisms proposed for the decomposition of ethyl and ethyl 3-phenyl glycidate.

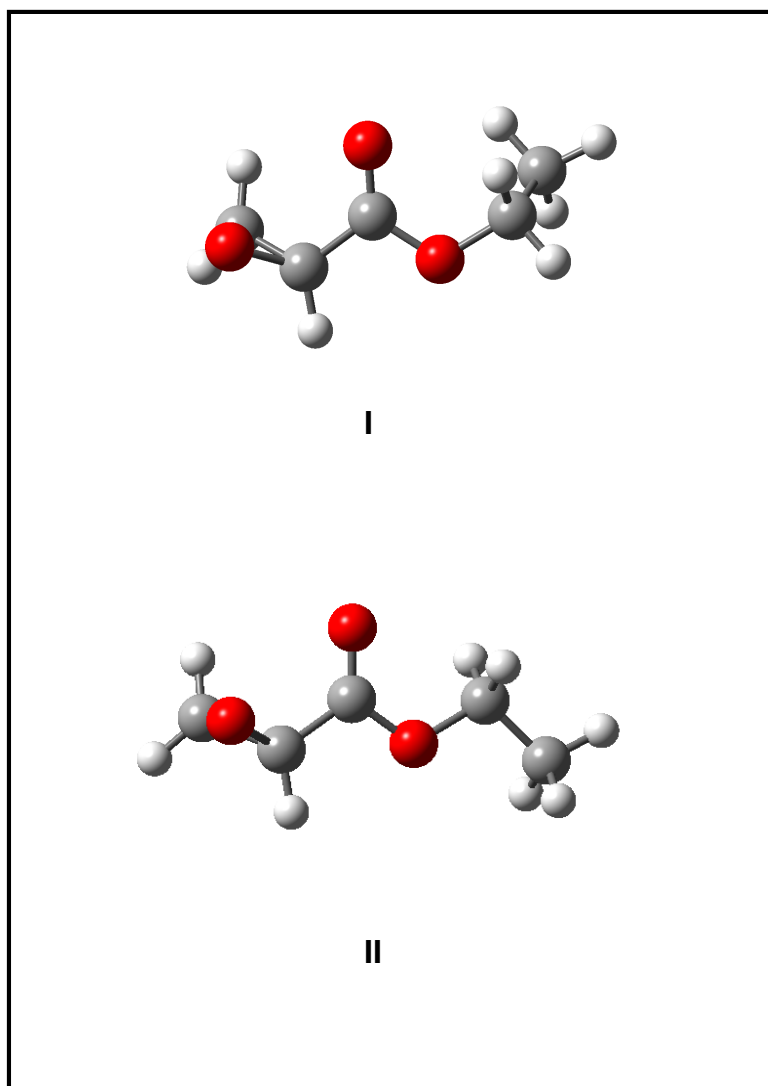
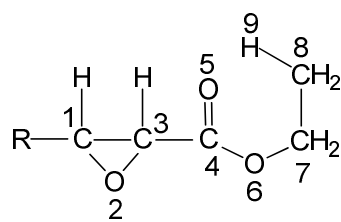


**Figure 2.** Geometry of ethyl glycidate minima at the MP2/6-31+G\* level.



R=H, C<sub>6</sub>H<sub>5</sub>

**Figure 3.** Atom numeration used in this work.

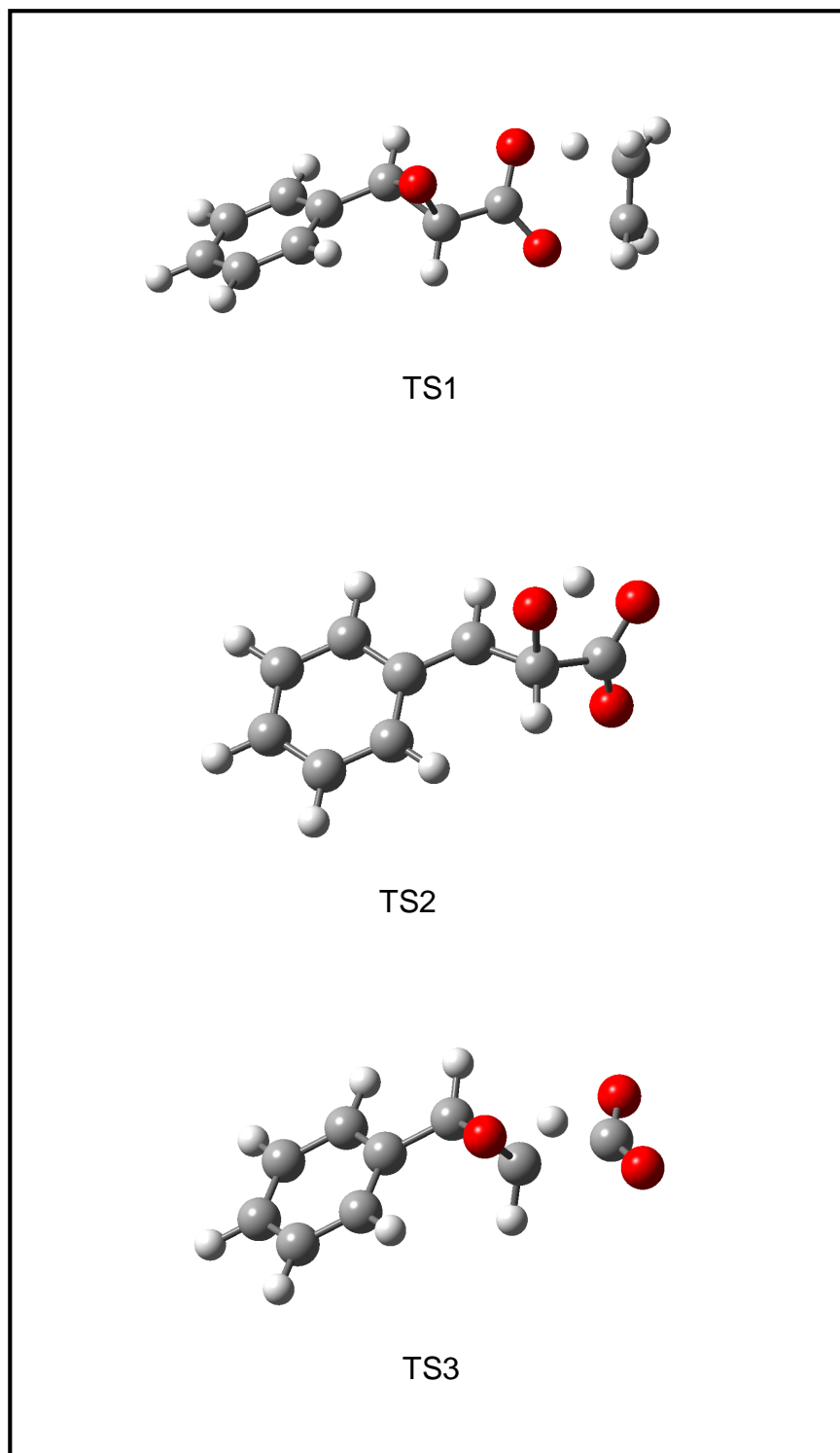


**Figure 4.** MP2/6-31+G\* geometry of the transition states; TS1 corresponding to the first step of the decomposition of ethyl 3-phenyl glycidate, TS2 and TS3 corresponding path I and path II for the second step of mechanism, respectively.

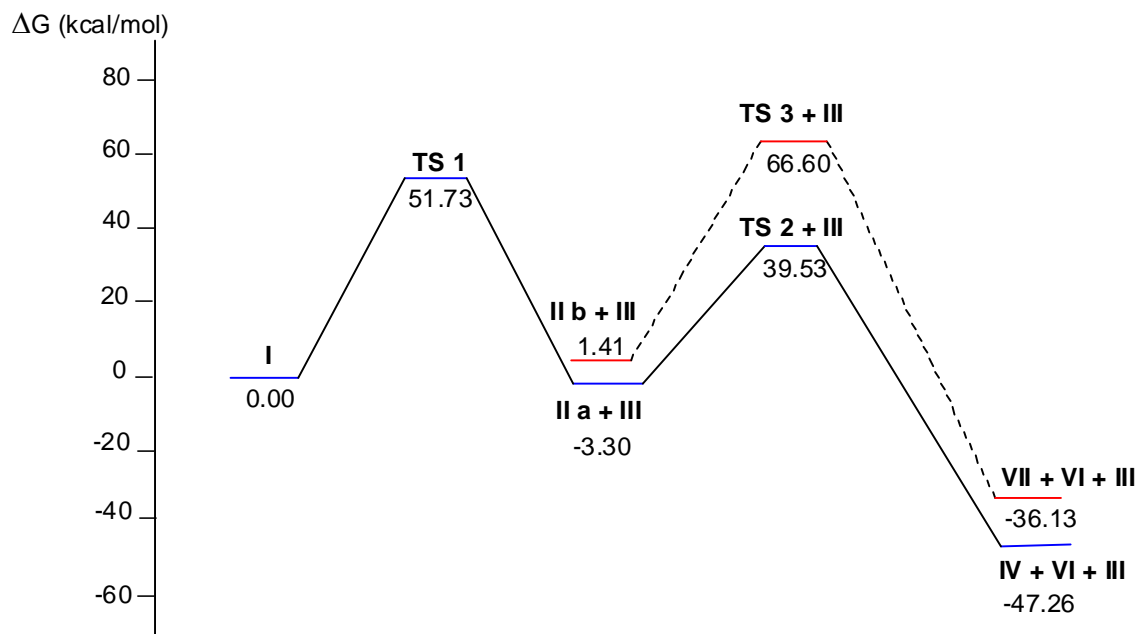


**Figure 5.** Gibbs free energy for the decomposition of ethyl 3-phenyl glycidate at the MP2/6-31+G\* level.

## References

- [1] Dullaghan, M.E.; Nord, F.F. *J. Org. Chem.* **1953**, 18, 878.
- [2] Blanchard, E.P.; Buchi, G. *J Am. Chem. Soc.* **1963**, 85, 955.
- [3] Shiner, V.J.; Martin, B. *J Am. Chem. Soc.* **1962**, 84, 4824.
- [4] Singh, S. P.; Kagan, J. *J. Org. Chem.* **1970**, 35, 2203.
- [5] Newman, M.S.; Magerlein, B.J. in *Organic Reactions*, vol.5. Wiley: New York, **1949**, 413.
- [6] Chuchani, G.; Tosta, M.; Rotinov, A.; Herize, A. *J. Phys. Org. Chem.* **2004**, 17, 694.
- [7] Notario, R.; Quijano, J.; Sánchez, C.; Vélez, E. *J. Phys. Org. Chem.* **2005**, 18, 134.
- [8] Chuchani, G.; Nuñez, O.; Marcano, N.; Napolitano, S.; Rodríguez, H.; Ascanio, J.; Rotinov, A.; Domínguez RM.; Herize. *J. Phys. Org. Chem.* **2001**, 14, 146.
- [9] Mirna, M.; Heredia, R.; Loroño, M.; Córdova, T.; Chuchani, G. *J. Mol. Struct. (THEOCHEM)*. **2006**, 770, 131.
- [10] Quijano, C.; Notario, R.; Quijano, J.; Sánchez, C.; León, L.; Vélez, E. *Theor. Chem. Acc.* **2003**, 110, 377.
- [11] Hölderich, W.F.; Barsnick, B. in: *Fine Chemicals through Heterogeneous Catalysis*, Sheldon, S.A.; Van Bekkum, H.; Eds.; Wiley-VCH, Germany, **2001**, 217.
- [12] Janes, D.; Kantar, D.; Kreft, S.; Prosen H. *Food Chem.* **2009**, 112, 120.
- [13] Tieman, D.; Schauer, N.; Fernie, A. R.; Hanson, A. D.; Klee, H. *J. Proc. Natl. Acad. Sci. USA*, **2006**, 103, 8287.
- [14] Wiberg, K.B. *Tetrahedron*. **1968**, 24, 1083.
- [15] Hermida-Ramón, J.M.; Rodríguez-Otero, J.; Cabaleiro-Lago, E.M. *J. Phys. Chem. A*. **2003**, 107, 1651.
- [16] Fukui, K. *J Phys Chem.* **1970**, 74, 4161.

[17] Gaussian 03, Revision C.02, Frisch, M. J.; Trucks, G. W.; Schlegel, H. B.; Scuseria, G. E.; Robb, M. A.; Cheeseman, J. R.; Montgomery, Jr., J. A.; Vreven, T.; Kudin, K. N.; Burant, J. C.; Millam, J. M.; Iyengar, S. S.; Tomasi, J.; Barone, V.; Mennucci, B.; Cossi, M.; Scalmani, G.; Rega, N.; Petersson, G. A.; Nakatsuji, H.; Hada, M.; Ehara, M.; Toyota, K.; Fukuda, R.; Hasegawa, J.; Ishida, M.; Nakajima, T.; Honda, Y.; Kitao, O.; Nakai, H.; Klene, M.; Li, X.; Knox, J. E.; Hratchian, H. P.; Cross, J. B.; Bakken, V.; Adamo, C.; Jaramillo, J.; Gomperts, R.; Stratmann, R. E.; Yazyev, O.; Austin, A. J.; Cammi, R.; Pomelli, C.; Ochterski, J. W.; Ayala, P. Y.; Morokuma, K.; Voth, G. A.; Salvador, P.; Dannenberg, J. J.; Zakrzewski, V. G.; Dapprich, S.; Daniels, A. D.; Strain, M. C.; Farkas, O.; Malick, D. K.; Rabuck, A. D.; Raghavachari, K.; Foresman, J. B.; Ortiz, J. V.; Cui, Q.; Baboul, A. G.; Clifford, S.; Cioslowski, J.; Stefanov, B. B.; Liu, G.; Liashenko, A.; Piskorz, P.; Komaromi, I.; Martin, R. L.; Fox, D. J.; Keith, T.; Al-Laham, M. A.; Peng, C. Y.; Nanayakkara, A.; Challacombe, M.; Gill, P. M. W.; Johnson, B.; Chen, W.; Wong, M. W.; Gonzalez, C.; and Pople, J. A.; Gaussian, Inc., Wallingford CT, 2004.

[18] Erickson, J.A.; Kahn, S.D. *J. Am. Chem. Soc.* **1994**, 116, 6271.

[19] Moyano, A.; Pericàs, M.A.; Valentí, E. *J. Org. Chem.* **1989**, 54, 573.

[20] Domingo, L. R.; Picher, M.T.; Safont, V.S.; Andrés, J.; Chuchani, G. *J. Phys. Chem. A* **1999**, 103, 3935.